

## **CONSTELLATION OF CUBESATS FOR REALTIME IONOSPHERIC E-FIELD MEASUREMENTS FOR GLOBAL SPACE WEATHER**

**Geoff Crowley**

Atmospheric & Space Technology Research Associates (ASTRA) LLC

[gcrowley@astraspace.net](mailto:gcrowley@astraspace.net)

**C. Fish, M. Pilinski, I. Azeem**

Atmospheric & Space Technology Research Associates (ASTRA) LLC

[cfish@astraspace.net](mailto:cfish@astraspace.net), [mpilinski@astraspace.net](mailto:mpilinski@astraspace.net), [iazeem@astraspace.net](mailto:iazeem@astraspace.net)

**C. Swenson**

Utah State University, Center for Space Engineering

[Charles.swenson@usu.edu](mailto:Charles.swenson@usu.edu)

### **ABSTRACT**

Inexpensive and robust space-weather monitoring instruments are needed to fill upcoming gaps in the Nation's ability to meet requirements for space weather specification and forecasting. Foremost among the needed data are electric fields, since they drive global ionospheric and thermospheric behavior, and because there are relatively few ground-based measurements. We envisage a constellation of CubeSats to provide global coverage of the electric field and its variability.

The DICE (Dynamic Ionosphere CubeSat Experiment) mission was a step towards this goal, with two identical 1.5U CubeSats, each carrying three space weather instruments: (1) double probe instruments to measure AC and DC electric fields; (2) Langmuir probes to measure ionospheric electron density, and; (3) a magnetometer to measure field-aligned currents. DICE launched in October 2011. DICE was the first CubeSat mission to observe a Storm Enhanced Density event, fulfilling a major goal of the mission.

In this paper we show the utility of a constellation of electric field measurements, describe the CubeSat and instrument suite that comprise the "SensorSat", and demonstrate how the measurements will meet or exceed the Nation's DoD and Civil space environment monitoring requirements. We will also present new CubeSat and Small Satellite space and ground segment technologies that are helping enable the practical implementation and management of CubeSat constellations, including low cost access to space, high speed space to earth communications, and global ground station networks.

## SYSTEMS SCIENCE

Systems science is an interdisciplinary field that studies the nature of complex systems in nature and science itself. It aims to develop interdisciplinary foundations that are applicable in a variety of areas [1]. An example of an area that would benefit from a systems science approach is the Ionosphere-Thermosphere-Mesosphere (ITM) region. The ITM serves as the cross-over boundary between Earth's heliophysical and atmospheric expanses in which both electro-dynamic and fluid-dynamic processes operate (reference Figure 1) and play an important role in Sun to Earth interactions and the overall energy budget of Earth's upper atmosphere. However, there are few measurements of the detailed coupling between these processes in this system and their global impact is still poorly understood [2; 3]. Few observations of the fields or state variables and their coupling are available, and hence no validation of the fundamental neutral or plasma processes has been accomplished.

The need for a better understanding of the ITM processes and their role in bridging the dynamics between the Earth's atmosphere and geospace through systems science has been highlighted in several NASA Heliophysics Roadmaps and Decadal Surveys. Future studies of the ITM region will require new observational paradigms that bring about a systems science perspective. The systems science approach implies the measurement of globally distributed effects, and therefore global, simultaneous, multi-point measurements. In turn, this implies multiple satellites making measurements at the same time. Using traditional approaches, the cost of multiple satellites would be prohibitive, thus an additional paradigm shift is required to smaller, simpler satellites. In this scenario, the space-based asset may well be a "one-instrument" miniature spacecraft platform, sometimes called a "Sensor-Sat", in order to reduce the cost of flying multiple satellites.

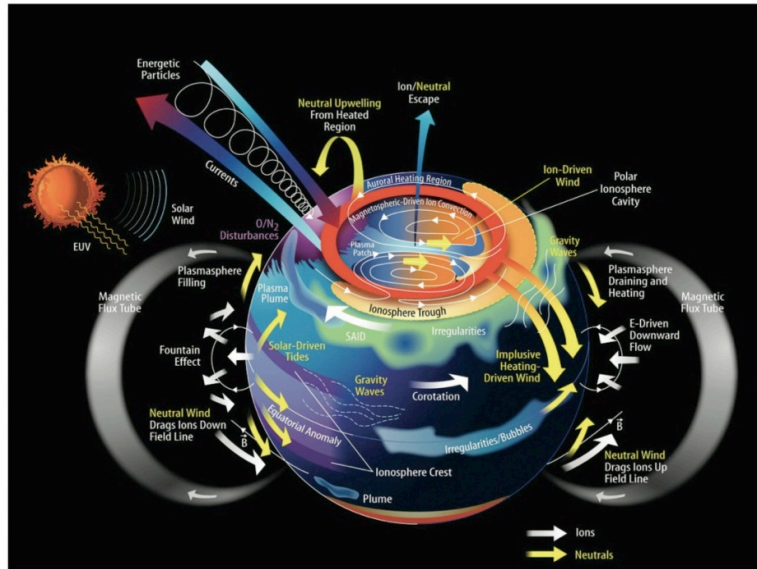


**Figure 1.** System view of dynamics and processes driven in ITM region due to coupling with drivers from the Sun and Earth's atmosphere (courtesy NASA).

## SYSTEM OBSERVATIONS FROM CONSTELLATIONS

Significant advances in Earth, solar, and space physics over the next decades will originate from new observational techniques. The most promising observation technique to still be fully developed is the capability to conduct multi-point or large distributed observations of the Earth system at a feasible cost. This approach is required to understand the "big picture", system-level coupling between disparate regions such as the solar-wind, magnetosphere, ionosphere, thermosphere, mesosphere, atmosphere, land, and ocean on a planetary scale. Multipoint measurements are also needed to develop understanding of the various scalars or vector field signatures (i.e gradients, divergence) that arise from coupling processes that occur across temporal and spatial scales within localized regions.

Remote ground based imaging is one approach to implement multi-point measurements of systems, but not all measurement parameters of interest can be observed through remote sensing techniques and it is also challenging to place ground based sites in certain points on the globe, such as throughout the ocean and in the polar regions. Some examples that are not well observed by remote imaging, in the ITM system for example, are electric field patterns and currents flowing along magnetic field lines. Both of these parameters are crucial to understanding the coupling of various regions. The details of atmospheric composition are also difficult to observe remotely but are an important parameter for the chemical dynamics of the lower ITM. The NASA Science Mission Directorate has repeatedly identified in recent roadmaps the pressing need for multipoint scientific investigations to be implemented via satellite constellations that enable both global *in-situ* and remote sensing observational options. The NASA Earth Science Division's "A-train" [4], consisting of Aqua, CloudSat, CALIPSO and Aura satellites, each with different sensors, is an example of such a constellation.

However, the costs to date of this and other proposed space-based constellations have been prohibitive given previous "large satellite" architectures and the multiple launch vehicles required for implementing the constellations. The resources that will be available over the next decades for all areas of scientific research and operational missions have limits. It is therefore important that the scientific and technical community find ways to leverage new technology developments to advance science. The high cost of access to space is a serious impediment to making multipoint measurements within the space environment (i.e., in deploying constellations of traditional satellites). It is therefore desirable to develop much smaller and lower-cost sensor/satellite systems such that the largest number of distributed measurements can be economically made in the space environment. The smaller the mass and volume of the sensor/satellite the larger the number will be that can be deployed from a single launch vehicle. The prospect of creating miniaturized sensors and satellite systems is positive given the enormous investment of commercial, medical, and defense industries in producing highly capable, portable and low-power battery-operated consumer electronics, *in-situ* composition probes, and novel reconnaissance sensors. The advancement represented by these technologies has direct application in developing small sensor/satellite systems for scientific research

Affordable constellations are not the only observational tool enabled by smaller and lower-cost sensor/satellite systems. With them it becomes feasible to put "almost disposable" platforms into heretofore sparsely or un-sampled locations or regions where it is currently not economical to place larger more expensive satellites. Deployed into very low Earth orbit, these small low-cost platforms could carry instruments into the lower ITM region. For instance, the region between 100 km and about 350 km in the Earth's atmosphere is not conducive to long lifetime orbits but could be monitored nearly continuously by periodically deploying small satellites from the International Space Station. This lower ITM region is where the full complexity of electro-dynamics and fluid-dynamics is exhibited, but where satellite drag ensures a quick end to satellite lifetimes. It has thus become known as the "inaccessible region". Small low-cost satellites can be placed into short lifetime trajectories lasting only a few weeks or months for scientific purposes which would not be feasible for larger more-expensive satellites.

## **CUBESAT REVOLUTION and LOW-COST ACCESS to SPACE**

Financially sustainable deployment of multi-spacecraft constellations can only be achieved through the use of small spacecraft and associated sensors that allow for multiple hostings per launch vehicle. As the first step to achieving that state, the revolution in commercial mobile and other battery powered consumer technology has helped enable researchers in recent years to build and fly very small yet capable satellites, principally CubeSats. The CubeSat standard for nano-satellites was developed in the late 1990's for the use of the academic community

in teaching space systems engineering to the next generation. It has since become widely accepted both internationally and by a broad spectrum of organizations due to the low-costs and relatively easy access to launch services, which have been engendered by the CubeSat standard. The distinguishing characteristics of the CubeSat community's success are the use of a mechanical standard for containerized launch services and the opportunistic pairing of picosatellites with launch vehicles that provide deployment containers. Current estimates place the number of CubeSat developers worldwide at over 100 including governments, industry and academia.

The CubeSat standard outlines a base "1U" nano-satellite, as shown in Figure 2, which has a volume of approximately one liter (10 cm cube) and a mass  $\leq 1.33$  kg, with scaling to larger CubeSats (i.e., 1.5U, 2U, 3U, 6U, etc.) then defined in terms of the baseline 1U [5]. Most CubeSat projects thus far have used modern high-performance commercial electronics components, rather than the more expensive and less capable space grade components, and targeted low earth orbit insertions with relatively short ( $< 1$  year) mission lifetimes.

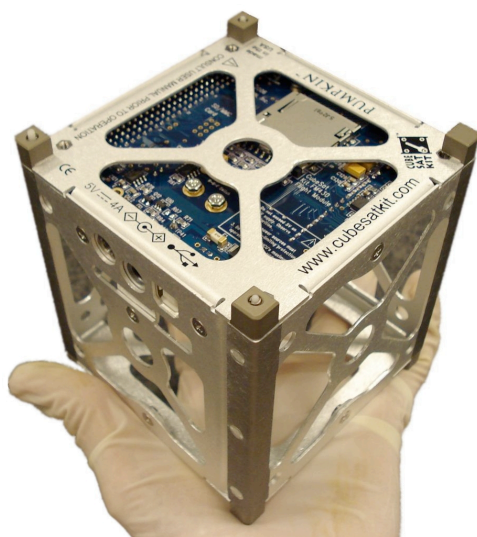


**Figure 2.** An example 1U CubeSat standard as defined in the Poly Picosatellite Orbital Deployer (P-POD) interface control document [5] (courtesy Pumpkin, Inc).

A majority of the CubeSat activity and development to date has come from international academia and the amateur radio satellite community, but several of the typical large-satellite vendors have begun to develop CubeSats as well. In 2004, CubeSats could each be fabricated and launched for as low as an estimated \$65,000–\$80,000 [6]. Recent government-sponsored CubeSat initiatives, such as the Air Force's Space Plug-N-Play Avionics program, the Operationally Responsive Space Office, the NRO Colony bus, NSF CubeSat Space Weather, NASA Office of Chief Technologist Edison and CubeSat Launch Initiative (CSLI) Educational Launch of Nanosatellites Educational Launch of Nano-satellites (ELaNa), ESA QB50, NASA Earth Science Technology Office In-Space Validation of Earth Science Technologies (InVEST), and the NASA Heliophysics Low Cost Access to Space (LCAS) programs have spurred the development of very proficient miniature spacecraft technologies that enable technology demonstration, space and earth science research, as well as opening the door for

operational CubeSat based missions. Recently, the interest from commercial groups has expanded dramatically, with commercial services now available from concept, to launch, and commercial data products.

## SENSOR REVOLUTION

In general, the development of CubeSat sized satellite infrastructure (step one in arriving at a state of launching many satellites/sensors from a single launch vehicle for constellation development) preceded the development of CubeSat compatible sensors (step two). However, contemporarily both CubeSat sized spacecraft and high end, science-grade, sensor technologies have been progressing in tandem. Much of that change has come from the recent establishment of regularly funded CubeSat based programs by government institutions around the world, as discussed above. The government sponsored CubeSat programs have introduced traceable requirements-driven designs which are implemented to achieve mission level objectives. This approach is the same as found on more traditional space research and operational programs. The miniature sizes of CubeSats has forced

tight integration of the spacecraft with the sensors, effectively creating “Sensor-Sats” for which the on-orbit spacecraft operations and performance are crucial to the performance of the sensors. This highly synergistic nature of the sensor-sat configurations quite often require ground testing and calibration of the sensors while integrated fully with the CubeSat platform. More recently, this forward progress has been strengthened even further by investments and utilization of sensor-sats by the commercial sector (e.g., Planet Labs Earth imaging [7]).

Highly capable CubeSat sensors are resulting from the recent worldwide uptick in sensor development across the science and now commercial communities. This quickened pace in sensor development is in response to the CubeSat satellite development revolution and the opportunity it has afforded to make multi-point measurements. Due to the great emphasis that has been placed globally on the development of sensor-sats, networked observations of systems is becoming ever more a reality and way of the future in space and earth science and operational missions. For example, the exciting ESA sponsored QB50 program will shortly (2016) launch a total of 50 sensor-sats, comprised of 2U and 3U CubeSat platforms, into a string-of-pearls configuration in the lower ITM that will provide systems science as well as a comprehensive understanding of CubeSat re-entry physics [8]. These developments also open the door for planetary missions, with considerations and designs for swarms of CubeSats encircling asteroids and distant planets already underway.

### NEED FOR GLOBAL SPACE WEATHER ELECTRIC FIELD MEASUREMENTS

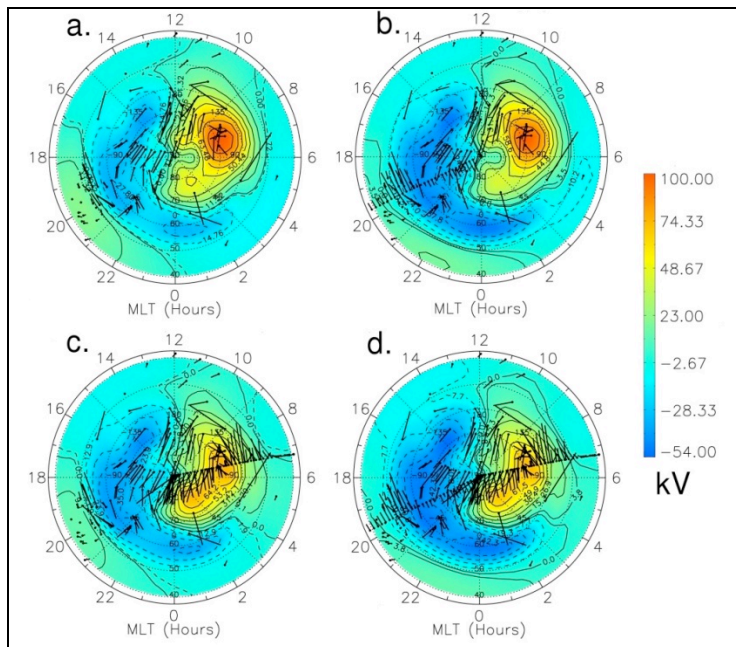


**Figure 3.** Northern hemisphere polar cap potential patterns (black contour lines) from AMIE for October 29, 2003 at 18:45 UT. All plots use Apex magnetic coordinates. Black arrows indicate measurements of ionospheric convection.  
a) only ground-based magnetometer data;  
b) ground-based magnetometers and ion drifts from DMSP F14 in the evening sector;  
c) ground-based magnetometers and DMSP F13 ion drifts in the dawn sector;  
d) ground-based magnetometers and both the F13 and F14 ion drifts.

Figure 3 illustrates the effect of varying data coverage from electric field (E-field) sensors for space weather assimilation purposes. Each electric potential distribution was obtained from the Assimilative Mapping of Ionospheric Electrodynamics (AMIE) algorithm [9, 10]. The black symbols represent the locations where data were available for ingestion into AMIE. These data include in-situ measurements from the DMSP satellite, SuperDARN coherent-scatter radar, and ground-based magnetometers. The precise shapes of the electric potential contours in the dawn and dusk sectors depend on which combination of datasets is ingested. There are many times when there is no DMSP data for ingestion. This hinders the specification of high latitude convection patterns and impedes one of the most important inputs to the global ionosphere and thermosphere (IT) system.

Without an accurate specification of the high latitude convection pattern, the global IT system cannot be predicted or specified by first-principles models. These data-gaps could be addressed in a cost-effective way by a constellation of CubeSats measuring electric

fields directly. The demonstration of E-field measurements from CubeSats will open up the possibility of a constellation to measure the spatial and temporal evolution of this important geophysical parameter. Table 1 shows the IORD-II requirements, which motivate the CubeSat electric field measurement evolution. Table 2 then lists the expected capabilities and relevant margins of the CubeSat based constellation using the Dynamic Ionosphere CubeSat Experiment (DICE) observatory and next generation Double-probe Instrumentation for Measuring Electric-fields (DIME) observatory design outlined in following sections.

<b>Quantity</b>	<b>Requirement</b>	<b>Goal</b>
Range	0-150 mV/m	0-250 mV/m
Precision	±2 mV/m	±0.1 mV/m
Accuracy	±3 mV/m	±0.1 mV/m
In-track Res.*	1.0 km	0.1 km

\*unspecified for E-field in IORD, using values from the IORD-II B-field requirements.

<b>Driving Requirement (Goal)</b>	<b>Capability</b>	<b>Margin (Goal)</b>
<b>E-Field (Satellite Ref Frame)</b>	<b>E-Field (Satellite Ref Frame)</b>	<b>E-Field</b>
1. ± 1250 (1250) mV/m range	1. ± 1625 mV/m range	1. 27% (26%)
2. 0.5 (0.15 ) mV/m sensitivity	2. 0.057 mV/m sensitivity	2. 908% (202%)
3. 3.6 (0.15) mV/m uncertainty	3. 1.96 mV/m uncertainty*	3. 14% (-49%) *
4. DC to 4 (50) Hz bandwidth	4. DC to 20 Hz bandwidth	4. 400% (-60%)
5. 4 to 1k (12k) Hz spectrum	5. 20 to 12k Hz spectrum	5. Meets Goal
6. 4 (16) spectrometer channels	6. 16 spectrometer channels	6. Meets Goal

\*Assuming an attitude uncertainty of 0.40°

## MODEL OBSERVATORIES – DICE and DIME

**DICE:** Sponsored by NSF CubeSat Space Weather and NASA ELaN program, the dual-spacecraft DICE mission exemplifies a next-generation advanced space research undertaking. DICE consists of a pair of 1.5U CubeSats launched into an eccentric low Earth orbit (LEO) on October 28, 2011, with each satellite equipped with instrumentation to measure ionospheric *in-situ* plasma densities, DC and AC electric fields, and DC and AC magnetic fields [11]. Each identical spacecraft carries two electric field probe pairs to measure *in-situ* DC and AC electric fields, two Langmuir probes to measure ionospheric *in-situ* plasma densities and temperature, and a complementary science grade magnetometer to measure *in-situ* DC and AC magnetic fields (see Figure 4 and Figure 5). The DICE spacecraft are orbiting at slightly differing velocities in nearly identical LEOs, permitting the de-convolution of

spatial and temporal ambiguities of ionospheric observations. The DICE mission is being enabled by a number of groundbreaking CubeSat technologies, including miniaturized mechanism actuators and software definable communications system operating at  $\geq 3$  Mbit/s. The total mass for each DICE observatory is just under 2.2 kg and they consume less than 1.9 W of on-orbit average power for all observatory functions.

The DICE Principal Investigator is Geoff Crowley, from ASTRA LLC. Charles Swenson, Utah State University, is the Deputy Principle Investigator. Chad Fish, ASTRA, is the Program Manager and a science Co-Investigator. Science team Co-Investigators include Marcin Pilinski, and Irfan Azeem from ASTRA and Aroh Barjatya from Embry Riddle Aeronautical University. The project lead engineer is Tim Neilsen, USU/SDL. ASTRA is leading mission science analysis, with support from USU/SDL and Embry Riddle. The DICE engineering component was implemented at USU/SDL, with support from ASTRA Inc. and Embry Riddle. Major engineering industry partners include L-3 Communications, TiNi Aerospace, Clyde Space, ATK Aerospace, and Pumpkin Inc. GPS simulator testing occurred at the NASA Goddard Space Flight Center. Mission operations are conducted by USU/SDL, in collaboration with NASA Wallops Flight Facility and SRI International.

The four electric field probe booms each extend 5 m from the spacecraft with electrically conductive spheres on the ends of the booms. The electric field probe booms are deployed via balance of mechanism lock force and centrifugal force resulting from a spin-up of the spacecraft. The Langmuir probe spheres are supported on the top and bottom of the spacecraft by the use of scissor booms that extend 13 cm away from the spacecraft. The bottom Langmuir probe boom, as well as a cutout in the bottom spacecraft panel, supports placement of a science grade



**Figure 4.** The DICE mission is a next-generation NSF and NASA-sponsored space research mission formed around CubeSat technologies.

magnetometer. The four shorter booms on the bottom-side of the spacecraft comprise the UHF communications turnstile antenna and are ~ 0.2 m in length. The UHF booms also increase the moment of inertia for the controlled spin of the spacecraft about the desired axis. Each sensor-sat consists of a frame manufactured from a single block of 7075 Aluminum. An isogrid pattern was used to maintain structural integrity while reducing the mass of the structure. The top and bottom panels (+Z and -Z faces) are also machined aluminum, with cutouts and mounting holes for release mechanisms, the Langmuir probes, GPS antenna, science magnetometer, and antenna mounts.

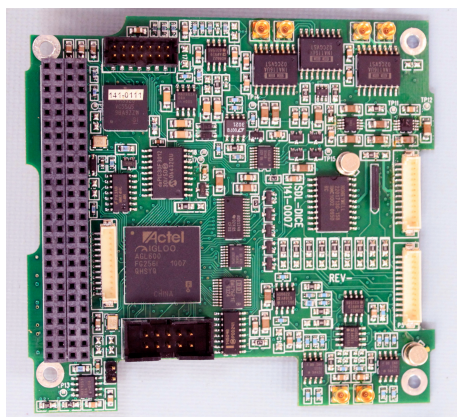
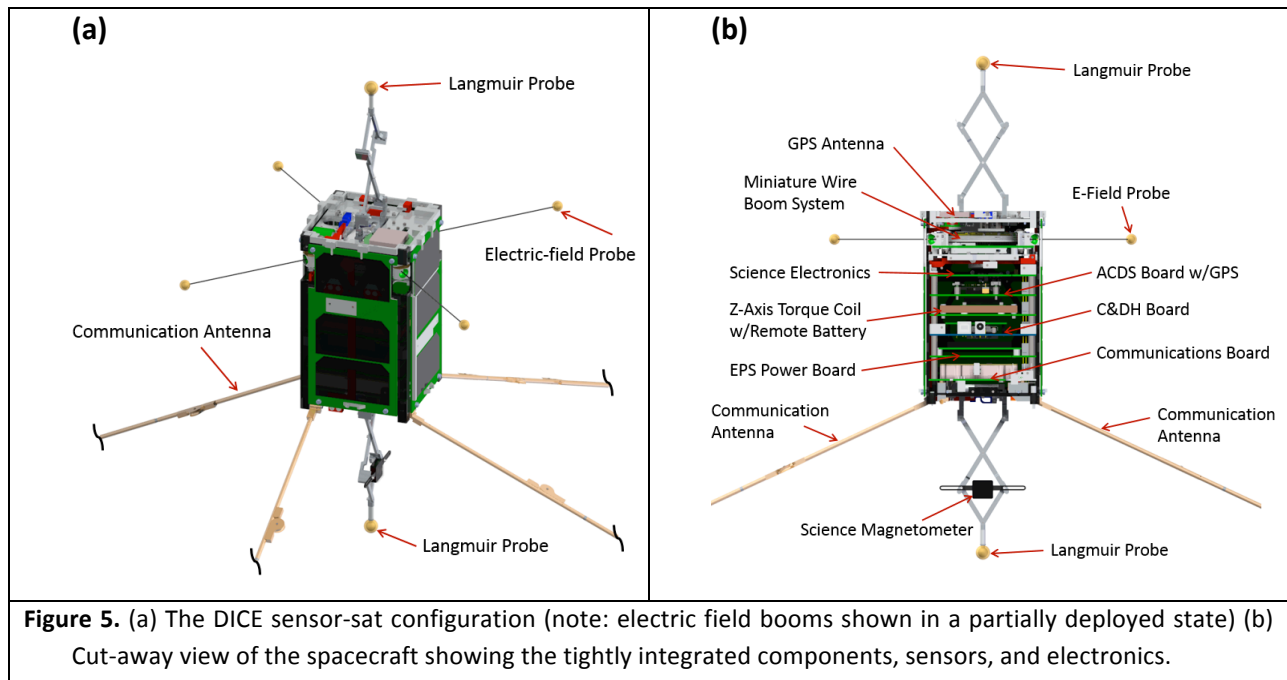


**Figure 6.** The DICE instrument suite electronics are all integrated onto one miniature PCB (~ 9.5 cm x 9.5 cm x 1.5 cm) that resides in the top of the DICE sensor-sat.

Electronics are mounted in a vertical stack (see Figure 5), and consist of, moving from the bottom of the stack up, 1) radio and antenna interface components, 2) electrical power system (EPS) that includes the primary battery, solar panel connections, and power system monitoring and conditioning electronics, 3) control and data handling (C&DH) electronics, 4) Z-axis torque coil and secondary battery electronics, 5) attitude control and determination system (ADCS) electronics that include interfaces to a sun sensor, ADCS magnetometer, GPS receiver, and the spacecraft torque coils (Z-axis in stack, X- and Y-axis embedded in solar panel circuit boards), and 6) science instrument electronics that include interfaces to the electric field probes (EFPs), Langmuir probes (LPs), and science magnetometer (SciMag) sensors. The EFP boom deployment mechanism is mounted above the electronics stack, along with the main release mechanism for the antennas and scissor booms. A GPS antenna is located on the top panel. Solar

panels with three solar cells each are attached on the long sides. A sun sensor views externally through a small cut out in one of the solar panels. An attitude determination magnetometer is located on the ADCS electronics board within the spacecraft. The use of magnetic materials in the design of the DICE spacecraft was restricted to minimize magnetic contamination of the SciMag measurements.

The EFP, LP, and SciMag instruments electronics are housed in the spacecraft on a single printed circuit board (PCB), as shown in Figure 6, weighing only 45 grams. The analog and digital sections of the board are physically isolated to minimize electro-magnetic interference (EMI) and RF coupling between signal measurement, data acquisition, and signal conditioning circuitry. When in full operation, the science PCB consumes ~ 0.5 W. An FPGA controls operation of the science instrument suite as well as data acquisition, digitization, time stamping, data formatting, and serial communications with the C&DH sub-system such that packets of data passed to the C&DH are merely stored in the telemetry buffer, ready for transmission by the radio. The DICE EFP, LP, and SciMag measurements are sampled simultaneously (< 90 ns phase delay between each multi-instrument measurement event) at either a 35 or 70 Hz rate. The science instrument measurements are oversampled at a 17.9 kHz rate and then co-added and decimated to improve signal to noise ratio (SNR) levels. The FPGA also controls the EFP boom deployment system. A summary of the DICE sensor performance is shown in Table 3.

<b>Table 3. DICE Requirement and Specification Listing</b>				
<b>Parameter</b>		<b>Requirement</b>		<b>Specification</b>
<b>E-Field Probe</b>				
Boom Length	≥	4	m	6
Range	≥	6.8	±V	13
Sensitivity	≤	2	mV	0.4
Uncertainty	≤	1	mV	0.2
DC Bandwidth	≥	4	Hz	35
<b>Floating Potential Probe</b>				
Range	≥	3.4	±V	6.5
Sensitivity	≤	2	mV	0.4
Uncertainty	≤	1	mV	0.2
DC Bandwidth	≥	4	Hz	35
<b>Magnetometer</b>				
Range	≥	6.00E+04	±nT	6.10E+04
Sensitivity	≤	5	nT	0.36
Uncertainty	≤	30	nT	2
DC Bandwidth	≥	4	Hz	35
<b>Sweeping Langmuir Probe</b>				
Voltage Sweep Range	≥	-1.02 to 1.29	V	-7 to + 7.0
Voltage Step	≤	19	mV	16
Current Range	≥	64 to -1.6	μA	
HG Channel			±μA	0.7
LG Channel			±μA	200

Current Sensitivity	≤	643	±pA	
HG Channel			±pA	21.4
LG Channel			±pA	6103
Current Uncertainty	≤	64	±pA	1
Temperature Range		300 to 5000	K	300 to 5000
DC Bandwidth	≥	4	Hz	35
<b>DC Ion Langmuir Probe</b>				
Bias Voltage	≥	-1.02	V	-1
Current Range		0.0 to -1.6	±μA	
HG Channel	≥		±μA	0.7
LG Channel	≥		±μA	200
Current Sensitivity	≤	643	±pA	1.0
Current Uncertainty	≤	64	±pA	1
Density Range		10 <sup>4</sup> to 10 <sup>7</sup>	p/cm <sup>3</sup>	7.27x10 <sup>3</sup> to 6.24x10 <sup>8</sup>
DC Bandwidth	≥	4	Hz	35
<b>E-Field Spectrometer (only a 512 Hz bandwidth was ultimately utilized on DICE)</b>				
Effective Sample Rate	≥	1024	Hz	6400
FFT Size	≥	1024	Points	1024
AC Bandwidth	≥	4 to 1k	Hz	9.6 to 3.2K
Channels	≥	4	#	16
Range	≥	10 to 20,000	(μV/m)·Hz <sup>-1/2</sup>	0.17 to 23,570
Sensitivity	≤	10	(μV/m)·Hz <sup>-1/2</sup>	0.17
Uncertainty	≤	10	(μV/m)·Hz <sup>-1/2</sup>	0.17
AC Boom Shielding		Full Cable Length		Full Length
<b>System Interface</b>				
Power	≤	0.4	W	0.33
Mass	≤	80	g	70
Internal Sampling Rate	≥	50	Hz	2.50E+04
Size		CubeSat Standard		
Telemetry Rate	≥	50	Hz	300
Comm Interface		UART		UART
Command and Control		External		External
Power Interface		Vbatt, 3.3/5VD		Vbat, 3.3/5VD
Operating Temperature	≤	-10	°C	-40
Operating Temperature	≤	40	°C	85

Figure 7 shows on-orbit LPS measurements made by the two DICE sensor-sats, which are appropriately named Yahtzee and Fark. The Yahtzee data is shown in panel a, while the Farkle data is shown in panel b. These plotted data are from the intermittent sweeps (i.e., Sweeping Langmuir Probe mode) which occur every 120 s and cover a voltage range from -4 to +1.7 VDC. The shapes of these raw low noise  $I$ - $V$  curves follow the projected responses and demonstrate that the LPs are operating as predicted. The difference in magnitude for the responses from the LPs on the same sensor-sat highlight that in general one of the LP sensors will be positioned more fully in the spacecraft velocity direction than the other. Thus, the higher current curves belong to the sensors that are in full or partial RAM, while the lower current curves belong to the sensors that are in a partial wake.

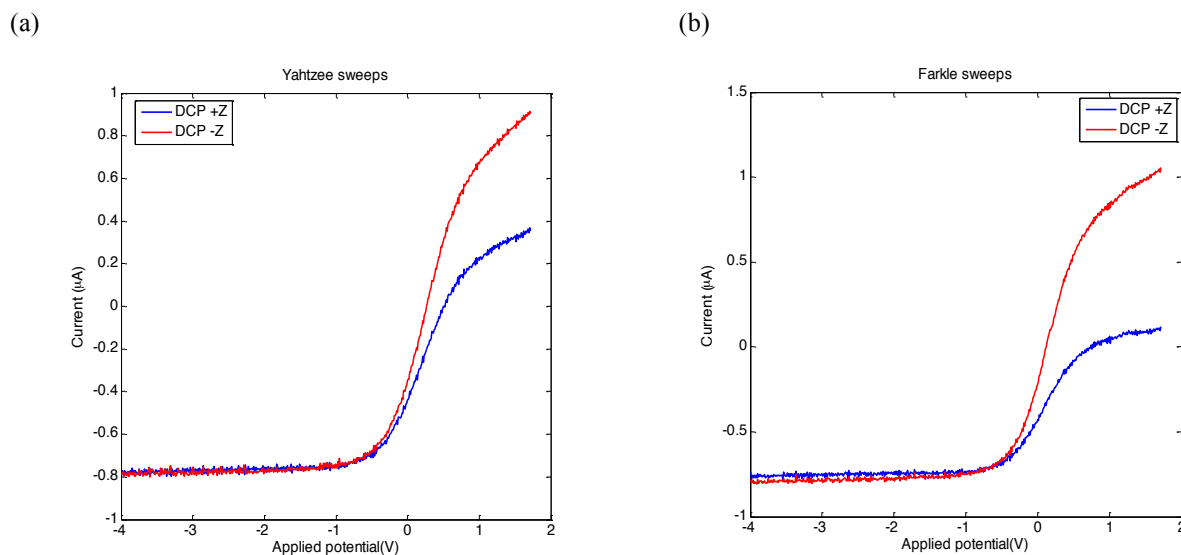


**Figure 7.** On-orbit  $I$ - $V$  curves generated by the DICE sensor-sat LPs.

Figure 8 compares multi-orbit Farkle LP data from June 29<sup>th</sup>, 2012 to outputs of two ionospheric weather models; namely the Ionospheric Reference Model (IRI), and ASTRA IDA4D model. IRI is a climatology model, while IDA4D is a nowcast assimilative model that updates on a regular basis, and is forced by ingested real-time observations. The ASTRA IDA4D assimilation used IRI 2007 as a background or starting point, and assimilated GPS TEC measurements, and COSMIC GPS radio occultation data. The DICE LP measurements exhibit general agreement with the established ionospheric model predictions, while also demonstrating fine structure detail.

The two top panels show the Yahtzee and Farkle measurements against the co-located model outputs. The bottom panel provides a global reference of the DICE sensor-sat measurement tracks on top of IDA4D generated ionospheric density outputs for 500 km. In making these plots, the two ion density DICE LP measurements for each spacecraft were averaged and then low-pass filtered and normalized to IDA4D model outputs. Once again, the DICE LP observations agree very well with the model outputs, while not unexpectedly providing greater resolution to the overall structure. These plots also help emphasize how simultaneous measurements of spacecraft in trailing orbits can help distinguish between temporal and spatial attributes of the ionosphere. Very similar structures are seen by both spacecraft as they go through nearly identical portions of the ionosphere. However, there is also enough orbital separation (nearly  $\frac{1}{2}$  an orbit for this time in the mission), that they also fly through different portions of the ionosphere at dissimilar times and provide perspective on global spatial structure and continuity.

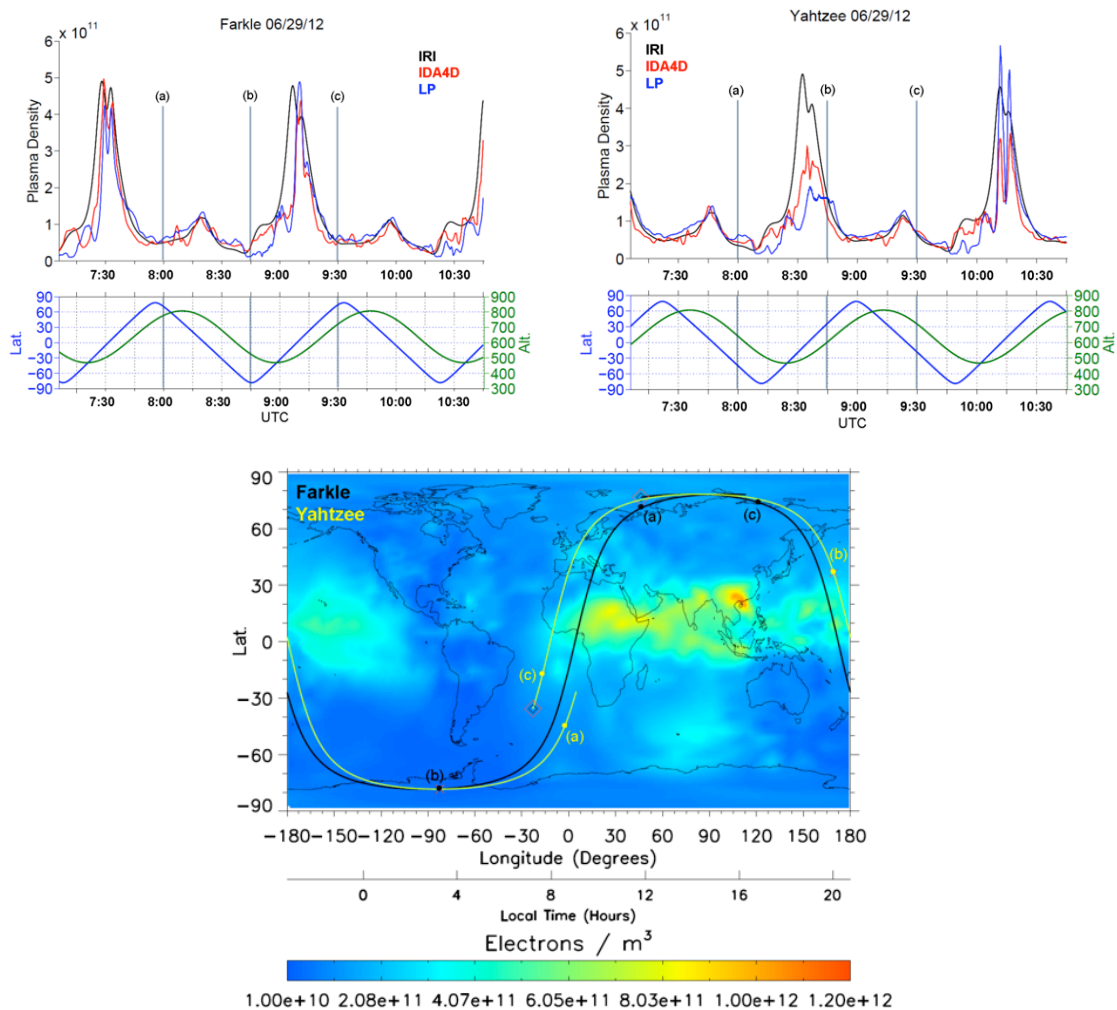


**Figure 8.** Comparison of simultaneous Farkle (top left) and Yahtzee (top right) LP measurements versus IRI and IDA4D model outputs for June 29<sup>th</sup>, 2012. The bottom panel shows a global IDA4D plasma density map for 500 km, with the DICE orbital tracks displayed for reference; the letter annotations in the bottom panel correspond to the correspondingly marked times in the upper two plots.

Next, Figure 9 investigates co-incident Yahtzee SciMag and ADCS magnetometer measurements acquired June 3, 2012. Figure 9 (panel a) demonstrates the very good, high level agreement in the measurements from the two sensors. As they should, the post-processed signals from both sensors lay directly on top of one another (see processing details below). Panel b is then a close up examination of a portion of the measurements, establishing the much lower noise floor of the SciMag measurements. The < 10 nT noise floor for the SciMag measurement enables detection and monitoring of geophysical disturbances and perturbations.

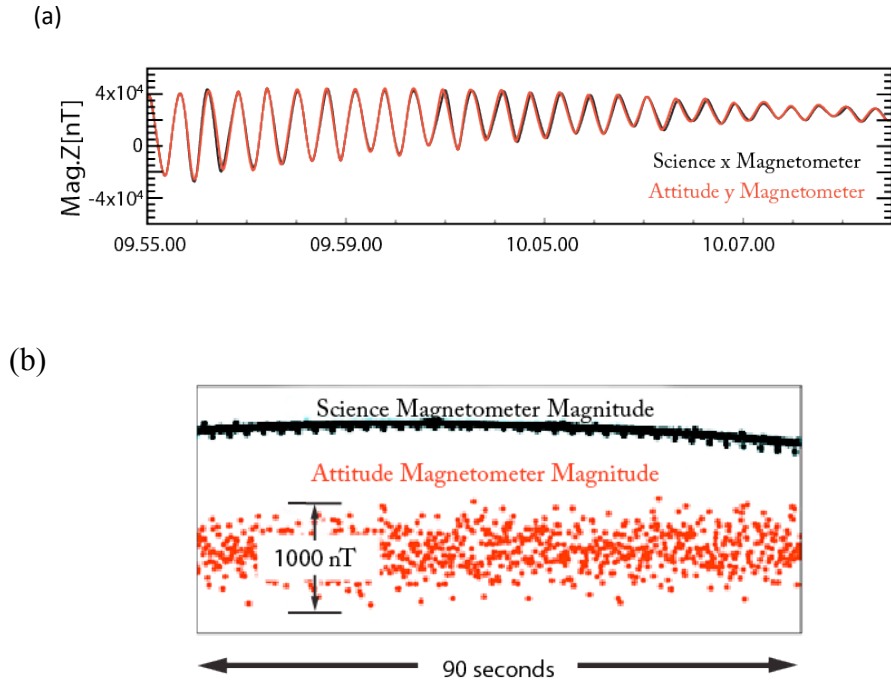


**Figure 9.** (a) Comparison of the DICE ADCS magnetometer and SciMag measurements on June 3, 2012. (b) A close up of the measurements, demonstrating the much lower noise ( $\sim 5\text{-}10$  nT) associated with the SciMag measurements.



**Figure 10.** The USU/SDL NOVA test facility is specially designed to allow for easy access and quick turnaround for CubeSat sized functional testing and system performance calibration activities

As part of the NASA ELaNa III program, the DICE spacecraft were required to undergo environmental qualification and launch specific functional testing. This testing focused on P-POD integrated testing and verification. Essentially, the integrated DICE P-POD assembly was required to demonstrate that there would not be any radio frequency, electrical power, or structural interference between DICE and the host launch vehicle during

launch as well as approximately one hour following ejection of DICE from the P-POD. Environmental testing included 1) structural random vibration, sinusoidal survey, and shock, and 2) thermal cycling and thermal vacuum bakeout. Non-ELaNa mission functional testing included “day in the life” operations verification, communication link budget and antenna pattern verification, mass properties verification, ADCS algorithm performance verification, and EPS performance verification testing. The communication link budget and antenna pattern verification occurred in collaboration with and at NASA WFF. Additionally, the DICE team utilized the USU/SDL Nano-satellite Operation Verification and Assessment (NOVA) facility (see Figure 10) which was critical to the functional and mass properties testing on DICE. The NOVA facility includes access to a walk-in Helmholtz cage, NIST traceable solar simulator, inertia and mass properties tables, Gauss chamber, and other hardware-in-the-loop utilities. This CubeSat-targeted test facility, along with the relative ease in handling CubeSat sized spacecraft, enabled quick turnaround testing and verification throughout the program. While many of the system level and environmental testing processes on DICE were similar to those followed for larger spacecraft missions, the miniature size of CubeSat platforms allows for quicker assembly and disassembly between test stations, easy transport and relocation by human handling or simple support equipment, and for parallel batch testing of many observatories in the same facilities.

Following the DICE mission, ASTRA (with Utah State University) is funded to build a follow-on proof-of-concept mission called DIME (Double-probe Instrumentation for Measuring Electric-fields), to further evaluate and demonstrate the use of spinning spacecraft and deployable wire booms to support Cubesat-based E-field measurements.

**DIME:** The DIME SensorSat (see Figure 11) design incorporates lessons learned from DICE mission operations [11], as well as from the DICE Attitude Determination and Control System (ADCS). Improvements in the Double Probe design are also being implemented. The DIME SensorSat is capable of deploying flexible electric field booms up to a distance of 10-m tip-to-tip and is capable of exceeding several IORD-2 threshold requirements. This is accomplished from the volume envelope of a 1.5U CubeSat, or 10x10x15cm. The satellite will measure AC and DC electric fields, together with ion densities, and magnetic fields to characterize the performance of the sensor in different plasma environments.

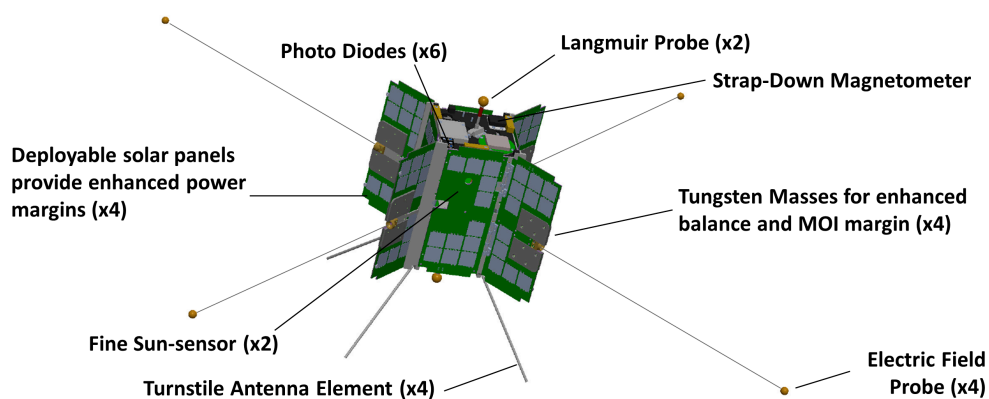


**Figure 11.** The DIME sensor-sat risk-reduction mission.

Since DIME is a risk-reduction mission, we plan to deploy the wire booms to 3 meter (6 meter tip-to-tip) lengths which will require pre-deployment spin rates of 1.5Hz. The box below lists the actuators and sensors used on DIME along with their placement and relationship to the spacecraft body frame. Note that the z-axis is the direction of nominal spin. The primary mission objective for DIMESat is: “Measure ionospheric electric-fields using

a wire-boom double-probe on a spinning CubeSat platform.” The minimum success criteria are (a) Deploy E-field booms and verify deployment on orbit and (b) Collect at least 50,000 minutes of E-field data on orbit.

In addition to having their own specific mission research objectives, DICE and DIME serve as pathfinders for low-cost, multi-point CubeSat constellation observations of the Sun-to-Earth system. Future expectations are for multiple copies of DIME-like spacecraft to be inserted into orbit to enable networked measurements of the interactions between the magnetosphere and ionosphere due to varying conditions originating on the sun. This will help provide a comprehensive understanding of the Earth’s global response to changing levels of solar activity. This constellation could contain up to 50-100 DIME CubeSats, all launched and inserted from a single vehicle, and able to acquire and transmit to ground nearly a Terabit of measurement data per day. This type of CubeSat-based constellation can be readily accommodated in the budget and programmatic constraints of a NASA Explorer program.

## MODELED RESULTS and EXPECTED FORECAST IMPROVEMENTS

One method for quantifying the value of electric field measurements is to examine the impact their assimilation has on specifying the neutral atmospheric state. This output is particularly important for nowcasting and predicting satellite drag for the myriad of resident space objects in low-earth orbit. Below, we compare model outputs from the TIME-GCM full-physics model when it is driven by assimilative convection patterns at high latitudes (AMIE procedure), an empirical high-latitude convection specification, and an empirical model of the neutral atmosphere with neutral density measurements from the CHALLENGING Minisatellite Payload (CHAMP) [12]. The TIME-GCM model is routinely driven by AMIE outputs at ASTRA, and has been used in many scientific studies [13, 14].

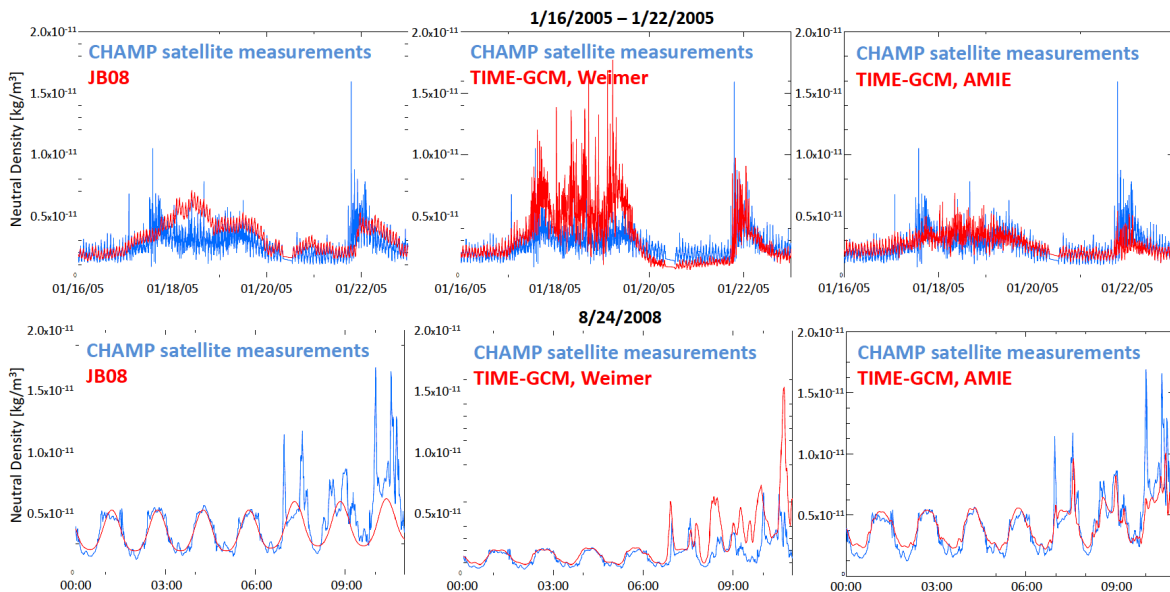


**Figure 12.** Improvements in neutral density when high-latitude electric fields are specified using assimilated electric fields.

Time-series of model and measured densities along the CHAMP satellite track are shown below (Figure 12) for three events (one event per row). The empirical model (the Jacchia Bowman or JB08) results are shown in the leftmost column. Results from TIME-GCM driven by an empirical [15] high-latitude convection pattern are shown in the center column. The rightmost column shows results from TIME-GCM when driven by an assimilative specification of high latitude convection (AMIE) including the ingestion of electric field measurements. The results demonstrate the improvement in the representation of high latitude density features when using AMIE with E-field assimilation. It is also seen that TIME-GCM driven by AMIE outperforms the empirical model (JB08) when specifying neutral densities.

## CONCLUSION

Over the next decades CubeSat sized science and operational observatories with sensor performance rivalling that of traditional systems will enable financially feasible implementations of global observational networks in space. These CubeSat based constellations will facilitate and allow the closing of key system science questions and provide operational platforms for both government and commercial ventures. In this paper we have reviewed two examples of small, low cost sensor technologies that have been developed or proposed for use on CubeSat observatories. We also explored how they are helping us do significantly more with less funding and technical resource allocations than was typically available on previous large satellite missions. These examples are only a small subset of the full body of work that is ongoing around the world. Indeed, the CubeSat spacecraft revolution and the subsequent revolution in science and earth-viewing sensor development are opening international doors of space science and operations that were only dreamed of before.

Although CubeSat technology is still progressing, major strides have been made in developing hardware infrastructure and instrumentation. DICE was a step in this evolution. It was the first scientific CubeSat constellation, and an ambitious program with each satellite carrying three space weather instruments. The mission had many successes, and there were also many lessons learned that are now being implemented in a follow-on called DIME. We anticipate that successes on DIME will pave the way forward to larger constellations, which will fill the present gaps in the nowcasting of ionospheric electrodynamics.

## REFERENCES

- [1] M'Pherson, P. K., A perspective on systems science and systems philosophy, *Futures* 6.3, 219-239, 1974.
- [2] Cosgrove, R. B., and M. Codrescu, Electric field variability and model uncertainty: A classification of source terms in estimating the squared electric field from an electric field model, *J. Geophys Res*, 114, A06301, 2009.
- [3] Thayer, J.P., and J. Semeter, The convergence of magnetospheric energy flux in the polar atmosphere, *J. of Atmospheric and Solar-Terrestrial Physics*, 66, 807–824, 2004.
- [4] [http://www.nasa.gov/mission\\_pages/a-train/a-train.html#.U2R4qFcvBJ0](http://www.nasa.gov/mission_pages/a-train/a-train.html#.U2R4qFcvBJ0)
- [5] CubeSat Design Specification, Rev. 13, California State Polytechnic University, <http://browncubesat.org/wp-content/uploads/2013/01/Cubesat-Reqs.pdf>, 2014.
- [6] L. David, CubeSats: Tiny Spacecraft, Huge Payoffs, <http://www.space.com/308-cubesats-tiny-spacecraft-huge-payoffs.html>, 2004.
- [7] <http://www.planet.com/>

[8] <https://www.qb50.eu/>

[9] Richmond, A. D., and Y. Kamide. Mapping Electrodynamic Features of the High-Latitude Ionosphere from Localized Observations: Technique, *J. Geophys. Res.*, Vol. 93, No. A6, pp. 5741–5759, 1988

[10] Crowley, G., and C. Hackert, Quantification of High Latitude Electric Field Variability, *Geophys Res. Lett.*, 28, 2783-2786, 2001.

[11] Fish, C. S. and DICE team, Design, Development, Implementation, and On-orbit Performance of the Dynamic Ionosphere CubeSat Experiment Mission, *Space Science Reviews*, 10.1007/s11214-014-0034-x, 2014.

[12] Sutton, E. K., R. S. Nerem, and J. M. Forbes (2007), Density and winds in the thermosphere deduced from accelerometer data, *J. Spacecraft and Rockets*, 44(6), 1210, doi:10.2514/1.28641.

[13] Crowley, G., A. Reynolds, J. P. Thayer, J. Lei, L.J. Paxton, A.B. Christensen, Y. Zhang, R.R. Meier, D.J. Strickland, Periodic Modulations in Thermospheric Composition by Solar Wind High Speed Streams, *Geophys. Res. Lett.*, 35, L21106, doi:10.1029/2008GL035745, 2008.

[14] Crowley, G., D. J. Knipp, K. A. Drake, J. Lei, E. Sutton, and H. Lühr (2010), Thermospheric density enhancements in the dayside cusp region during strong  $B_y$  conditions, *Geophys. Res. Lett.*, 37, L07110, doi:10.1029/2009GL042143

[15] Weimer, D. R., Improved ionospheric electrodynamic models and application to calculating Joule heating rates, *J. Geophys. Res.*, 110, A05306, doi:10.1029/2004JA010884, 2005